Neuroimaging of astroblastomas: a case series and systematic review

Running title: Neuroimaging features of astroblastoma

Ryo Kurokawa[1], Akira Baba[1], Mariko Kurokawa[1], Yoshiaki Ota[1], Omar Hassan[1], Aristides Capizzano[1], John Kim[1], Timothy Johnson[2], Ashok Srinivasan[1], Toshio Moritani[1]

[1]Division of Neuroradiology, Department of Radiology, University of Michigan, 1500 E. Medical Center Dr., Ann Arbor, MI, 48109, US.

[2] Department of Biostatistics, University of Michigan School of Public Health, 1415 Washington Heights, Ann Arbor, MI, 48109, US.

* Corresponding author

Ryo Kurokawa, M.D., Ph.D.

Division of Neuroradiology, Department of Radiology, University of Michigan, Ann Arbor, Michigan

1500 E Medical Center Dr, UH B2, Ann Arbor, MI 48109.

Email: kuroro63@gmail.com

Phone: +1-784-219-2884

Fax: +1-734-615-9800

Funding: none.

Keywords: astroblastoma; neuroimaging features; CT; MRI; systematic review

Abstract

Background and Purpose

Astroblastoma is a rare type of glial tumor, histologically classified into two types with different prognoses: high and low grade. We aimed to investigate the CT and MRI findings of astroblastomas by collecting studies with analyzable neuroimaging data and extracting the imaging features useful for tumor grading.

Methods

We searched for reports of pathologically proven astroblastomas with analyzable neuroimaging data using PubMed, Scopus, and Embase. Sixty-five studies with 71 patients with astroblastomas met the criteria for a systematic review. We added eight patients from our hospital, resulting in a final study cohort of 79 patients. The proportion of high-grade tumors was compared in groups based on the morphology (typical and atypical) using Fisher's exact test.

Results

High-and low-grade tumors were 35/71 (49.3%) and 36/71 (50.7%), respectively. There was a significant difference in the proportion of high-grade tumors based on the tumor morphology (typical morphology: high-grade = 33/58 [56.9%] vs. atypical morphology, 2/13 [15.4%], p =

0.012). The reviews of neuroimaging findings were performed using the images included in each article. The articles had missing data due to the heterogeneity of the collected studies.

Conclusions

Detailed neuroimaging features were clarified, including tumor location, margin status, morphology, CT attenuation, MRI signal intensity, and contrast enhancement pattern. The classification of tumor morphology may help predict the tumor's histological grade, contributing to clinical care and future oncologic research.

Introduction

Astroblastoma is a rare tumor of glial origin, accounting for 0.45–2.8% of all gliomas.[1] It affects female children and adolescents more frequently.[2] Astroblastomas mainly develop in the supratentorial regions, but may also occur in the ventricles,[3,4] brainstem,[5] cerebellum,[6] and spinal cord.[7]

Clinically, patients with astroblastomas often present with headaches. Other common symptoms include seizures, focal neurologic deficits, and vomiting.[8,9] Cunningham et al. reported that a well-demarcated, solid, cystic, and enhanced masses with peritumoral edema were typical imaging features for astroblastomas.[10]

These tumors have been histologically classified into two types: low-grade/well-differentiated and high-grade/anaplastic based on the degree of cellularity, nuclear atypia, mitotic index, microvascular proliferation, necrosis (possibly with pseudopalisades), and the MIB-1 proliferative index.[11] Previous studies have reported that histological grouping correlates with prognosis.[12,13] However, the CT and MRI features useful to differentiate between the two grades have not been established. Although no study has focused on the relationship between the tumor morphology and grades, we noticed that astroblastomas could be classified into the several morphological types from clinical experience.

The purpose of this systematic review was to investigate the imaging features of astroblastoma by collecting previous studies with analyzable neuroimaging data and extracting the features useful for grading. It presents the largest cohort with analyzable CT and MRI images, including 79 cases.

Methods

This study was performed according to the Preferred Reporting Items for Systematic Reviews and Meta-Analyses (PRISMA) 2020 statement.[14]

Study selection

We searched studies published after 2001 in PubMed, SCOPUS, and Embase databases on July 14, 2021, without any language limit, using the following search words:

1. ("astroblastoma") AND ((radiology) OR (neuroradiology) OR (imaging) OR (magnetic resonance) OR (computed tomography)) for PubMed;
2. ALL (astroblastoma AND [(radiology OR neuroradiology OR imaging OR [magnetic AND resonance] OR [computed AND tomography]) for SCOPUS;
3. astroblastoma AND (radiology OR neuroradiology OR imaging OR [magnetic AND resonance] OR [computed AND tomography]) for Embase.

Eligible publications fulfilled the following criteria:

1. The tumors were histologically proven intracranial astroblastomas;
2. Analyzable preoperative CT or MRI images;
3. Each patient's demographic data were available.

The exclusion criteria were:

1. Only post-surgical status for astroblastoma;
2. Coexistence of other tumors;

3. Image quality insufficient for evaluation;

4. Unavailable full text.

Non-English articles were translated into English using Google Translate (www.translate.google.com) and examined. We obtained an exemption from our institutional review board to include unpublished cases from our hospital with histologically proven astroblastomas and preoperative CT and MRI images. We searched the electronic database of our institution without a date limit and found 14 patients with histologically proven astroblastomas. Among them, preoperative neuroimaging examinations were analyzable in eight patients meeting the inclusion criteria. Data were acquired in compliance with all applicable Health Insurance Portability and Accountability Act regulations.

Data analyses

Two board-certified radiologists with nine and six years of experience in neuroradiology, blinded to the tumor-grade, independently performed the study selection and CT and MRI image review. For numerical factors, the mean of the values between the two reviewers was used for the analyses. Any discrepancy in the categorical factors between the two reviewers

was arbitrated by a third board-certified radiologist with 13 years of experience in neuroradiology.

Collected data

The following data were collected:

Demographic:

- Patient age at diagnosis; sex.

Clinical:

- Presenting complaint; tumor grade; treatment strategy; recurrence after gross total resection; period between the initial surgery and tumor recurrence; survival status within the follow-up period in each study; follow-up duration.

Radiological:

- Tumor size, laterality, location, margin status, and morphology (four types, Figure 1); signal intensity of solid and cystic components (relative to the cortex) in T2-weighted images (T2WI), fluid-attenuated inversion recovery (FLAIR), and T1-weighted images

(T1WI); contrast enhancement; diffusion restriction and apparent diffusion coefficient (ADC) values; peritumoral edema; CT attenuation (relative to the cortex); intratumoral calcification; intratumoral hemorrhage. For ADC measurement, we placed three separate ROIs in the solid components of the tumors while carefully avoiding cystic, necrotic, calcified, or hemorrhagic regions and vessels. The mean was used for the analyses.

The description of the following factors from each study was extracted and included:

- The contrast enhancement pattern on post-enhanced T1WI when pre-enhanced T1WI were not analyzable;
- Calcification or hemorrhage in inconclusive images.

Quality assessment

We employed a tool to evaluate the methodological quality of case reports/series proposed by Murad et al.,[15] comprising eight signaling questions in four domains: selection, ascertainment, causality, and reporting.

Statistical analysis

The proportion of high-grade tumors was compared between groups based on the recurrence after gross total resection, tumor margin status, and morphology (typical and atypical) using Fisher's exact tests. The age at diagnosis was compared between the two tumor grades using Mann-Whitney U-test. The two most frequent tumor morphological types out of the four were considered typical, while the other two types were considered atypical. Family-wise error-corrected two-sided P values < 0.05 (Bonferroni) were considered statistically significant. We used the intraclass correlation coefficient (2, 1) and kappa analyses to assess the inter-reader reliability for the numerical and categorical factors, respectively. All statistical analyses were performed using R software (version 4.0.0; R Foundation for Statistical Computing, Vienna, Austria).

Results

Study selection

Database searches using PubMed, SCOPUS, and Embase yielded 265 abstracts which were screened using the PRISMA 2020 guidelines.[14] After removing duplications, irrelevant studies by title and abstract screening, and studies with unavailable full text, 101 potentially eligible studies remained. We excluded 36 studies based on the inclusion/exclusion criteria. We identified 65 studies, including 71 patients with astroblastomas, meeting the requirements of the systematic review (Figure 2),[1–6,10,12,16–72] ranging from 2002 to 2021. In addition, we included the unpublished reports of eight patients with astroblastomas from our hospital (Table 1), resulting in a final study cohort of 79 patients. MN1 expression was reported in nine cases from seven studies.[2,16–21]

Risk of bias assessment

Selection: The selection methods were rarely described in the studies since they were case reports and series. Therefore, selection bias may have been introduced.

Ascertainment: Treatment options and outcomes were ascertained in most cases.

Causality: The follow-up duration in surviving patients ranged from one month to over 11 years, which may impact the generalizability of the survival rates.

Reporting: CT, T2WI, FLAIR, pre-contrast T1WI, ADC values, and post-contrast MRI were analyzable in 27/79 (34.2%), 53/79 (67.1%), 30/79 (38.0%), 8/79 (10.1%), and 64/79 (81.0%), respectively.

Demographic and clinical data

The demographic and clinical data of the 79 patients are summarized in Table 2. The median age at diagnosis was 13 years (range: 0–77 years), with female predominance (62/79, 78.5%). The majority of patients were aged < 10 years (27/79, 34.2%), followed by 10–19 years (25/79, 31.6%). High-and low-grade tumors were observed in 35/71 (49.3%) and 36/71 (50.7%) patients, respectively.

The majority of the patients (51/75, 68.0%) presented with headaches, followed by nausea/vomiting (22/75, 29.3%), and seizure/epilepsy (20/75, 26.7%). Surgery alone was the most commonly employed option (44/76, 57.9%), and tumor recurrence after gross total resection was observed in 16/56 cases (28.6%). During the follow-up period, 58/68 patients (85.3%) survived (median, 18 months; range, < 1–135 months).

Neuroimaging data

The neuroimaging findings are summarized in Table 3. The majority of tumors were located in the supratentorial compartment (74/79, 93.7%). Tumor morphology I (24/79, 30.4%) and II (40/79, 50.6%) were considered typical, in contrast to atypical morphology III (8/79, 10.1%) and IV (7/79, 8.9%). Contrast enhancement was observed in all but one case (63/64, 98.4%). Diffusion restriction was observed in 9/14 patients (64.3%), with a median ADC value of 0.69 $\times 10^{-3}$ mm^2/s. Intratumoral calcification and hemorrhage were observed in 21/30 (70.0%) and 12/23 (52.2%) cases, respectively (patient 1, Figure 3). Dynamic susceptibility-enhanced perfusion MRI was performed in three cases,[2,25] including one of our patients (patient 8, Figure 4). Elevated cerebral blood flow and volume were observed in all cases. Representative cases from our hospital are shown in Figures 3–6. The inter-reader reliability was generally good (Table 4).

Statistical analyses

There was a significant difference in the proportion of high-grade tumors based on the tumor morphology (typical morphology [I or II]: high-grade = 33/58 [56.9%] vs. atypical

morphology [III or IV]: 2/13 [15.4%], p = 0.012), without significant differences in the other factors (Table 5).

Discussion

This systematic review investigated the demographic, clinical, and neuroimaging findings of 71 patients with astroblastomas with analyzable CT/MRI images in 65 publications and eight patients from our hospital. Astroblastomas were frequently located in the supratentorial regions (73/79, 92.4%). Patients under the age of 20 were mainly affected (52/79, 65.8%), with a female predominance (62/79, 78.5%). A significant difference emerged in the proportion of high-grade tumors based on the tumor morphology.

According to the 2016 World Health Organization (WHO) classification, astroblastomas are classified similarly to other neuroepithelial tumors, including choroid gliomas of the third ventricle and angiocentric gliomas.[73] Recent advances in the molecular understanding of CNS tumors revealed that *MN1* alteration is characteristic of tumors exhibiting the morphology and clinical characteristics of astroblastomas.[74] However,

astroblastoma diagnosis was based on histological features in most previous studies. Astroblastomas have generally been recognized in two different histological types: low-grade/well-differentiated and high-grade/anaplastic. High-grade tumors show a higher rate of progression and recurrence.[8,13]

Regarding radiological findings, Cunningham et al.[10] summarized the neuroimaging characteristics of 127 astroblastomas. They reported that typical neuroimaging findings of astroblastoma are the supratentorial and superficial locations, well-demarcated, mixed cystic-solid masses, and contrast enhancement. The tumor location and the frequency of contrast enhancement are consistent with our results. In this study, we restricted the study cohort to cases with analyzable CT/MRI images, providing two major advantages. It allowed us to evaluate imaging findings, such as CT attenuation, MRI signal intensity, and tumor margin status, using uniform criteria. Additionally, three board-certified radiologists reviewed and diagnosed the images in every case. Thus, several differences emerged between the study by Cunningham et al. and this study.[10] We identified 18/79 (22.8%) tumors with ill-defined margins, whereas only 3/82 cases (3.7%) were reported in their study.[10] We could evaluate the signal intensity of the cystic components of the tumors not examined previously. Furthermore,

we found a significant difference in the proportion of high-grade astroblastomas between the two categories considered on examining the tumors based on four morphologies. Considering the difference in the prognosis and recommended treatment strategy between high-and low-grade astroblastomas, this neuroimaging morphological classification may improve the clinical practice and promote further oncologic investigations.

This study had some limitations. Although this study presents the largest cohort of astroblastomas with analyzable CT/MRI images, the number of patients was limited. The reviews of neuroimaging findings were performed using the images included in each article, not the serial image slices. However, radiological evaluation was performed by three board-certified radiologists to mitigate the risk of inappropriate assessments. In addition, some data were missing due to the heterogeneity of the studies collected, including tumor size and findings of advanced MRI sequences, such as perfusion MRI and MR spectroscopy. Further studies with these advanced sequences are required.

In conclusion, astroblastoma frequently occurs in supratentorial regions in female patients under 20 years of age. By reviewing cases with analyzable CT/MRI images, detailed neuroimaging features were better characterized, including tumor location, margin status, morphology, CT attenuation, MRI signal intensity, and contrast enhancement pattern. The classification based on tumor morphology may help predict the tumor's histological grade, contributing to clinical care and future oncologic research.

Acknowledgements and Disclosure

We would like to thank Editage [http://www.editage.com] for editing and reviewing this manuscript for English language.

The authors declare that they have no competing interests.

References

1. Navarro R, Reitman AJ, de León GA, et al. Astroblastoma in childhood: pathological and clinical analysis. Childs Nerv Syst 2005;21:211–20.

2. Mhatre R, Sugur HS, Nandeesh BN, et al. MN1 rearrangement in astroblastoma: study of eight cases and review of literature. Brain Tumor Pathol 2019;36:112–20.

3. Yeo JJY, Low YYS, Putti TC, et al. Adult intraventricular astroblastoma. Singapore Med J 2016;57:53–4.

4. Denaro L, Gardiman M, Calderone M, et al. Intraventricular astroblastoma. Case report. J Neurosurg Pediatr 2008;1:152–5.

5. Notarianni C, Akin M, Fowler M, et al. Brainstem astroblastoma: a case report and review of the literature. Surg Neurol 2008;69:201–5.

6. Yapıcıer Ö, Demir MK, Özdamarlar U, et al. Posterior fossa astroblastoma in a child: a case report and a review of the literature. Childs Nerv Syst 2019;35:1251–5.

7. Yamasaki K, Nakano Y, Nobusawa S, et al. Spinal cord astroblastoma with an EWSR1-BEND2 fusion classified as a high-grade neuroepithelial tumour with MN1 alteration. Neuropathol Appl Neurobiol 2020;46:190–3.

8. Thiessen B, Finlay J, Kulkarni R, et al. Astroblastoma: does histology predict biologic behavior? J Neurooncol 1998;40:59–65.

9. Yunten N, Ersahin Y, Demirtas E, et al. Cerebral astroblastoma resembling an extra-axial neoplasm. J Neuroradiol 1996;23:38–40.

10. Cunningham DA, Lowe LH, Shao L, et al. Neuroradiologic characteristics of astroblastoma and systematic review of the literature: 2 new cases and 125 cases reported in 59 publications. Pediatr Radiol 2016;46:1301–8.

11. Salvati M, D'Elia A, Brogna C, et al. Cerebral astroblastoma: analysis of six cases and critical review of treatment options. J Neurooncol 2009;93:369–78.

12. Janz C, Buhl R. Astroblastoma: report of two cases with unexpected clinical behavior and review of the literature. Clin Neurol Neurosurg 2014;125:114–24.

13. Bonnin JM, Rubinstein LJ. Astroblastomas: a pathological study of 23 tumors, with a postoperative follow-up in 13 patients. Neurosurgery 1989;25:6–13.

14. Page MJ, McKenzie JE, Bossuyt PM, et al. The PRISMA 2020 statement: an updated guideline for reporting systematic reviews. BMJ 2021;372:n71.

15. Murad MH, Sultan S, Haffar S, et al. Methodological quality and synthesis of case series and case reports. BMJ Evid Based Med 2018;23:60–3.

16. Chadda KR, Holland K, Scoffings D, et al. A rare case of paediatric astroblastoma with concomitant MN1-GTSE1 and EWSR1-PATZ1 gene fusions altering management. Neuropathol Appl Neurobiol 2021;47:882–8.

17. Fudaba H, Momii Y, Kawasaki Y, et al. Well-differentiated astroblastoma with both focal anaplastic features and a Meningioma 1 gene alteration. NMC Case Rep J 2020;7:205–10.

18. Petruzzellis G, Alessi I, Colafati GS, et al. Role of DNA methylation profile in diagnosing astroblastoma: a case report and literature review. Front Genet 2019;10:391.

19. Burford A, Mackay A, Popov S, et al. The ten-year evolutionary trajectory of a highly recurrent paediatric high grade neuroepithelial tumour with MN1:BEND2 fusion. Sci Rep 2018;8:1032.

20. Hirose T, Nobusawa S, Sugiyama K, et al. Astroblastoma: a distinct tumor entity characterized by alterations of the X chromosome and MN1 rearrangement. Brain Pathol 2018;28:684–94.

21. Shin SA, Ahn B, Kim S-K, et al. Brainstem astroblastoma with MN1 translocation. Neuropathology 2018;38:631–7.

22. D Cruze L, Sundaram S, Iyer S, et al. A rare case of a high-grade astroblastoma with 5-year follow-up. Asian J Neurosurg 2021;16:183–6.

23. Sarper B, Yaprak Bayrak B, Halis H, et al. Malignant astroblastoma. Balkan Med J 2020;37:224–5.

24. Bernasconi R, Eccher A, Girolami I, et al. Extra-axial anaplastic astroblastoma in a 67-year-old woman. Neuropathology 2019;39:307–12.

25. Bhalerao S, Nagarkar R, Adhav A. A case report of high-grade astroblastoma in a young adult. CNS Oncol 2019;8:CNS29.

26. Majd NK, Metrus NR, Santos-Pinheiro F, et al. RBM10 truncation in astroblastoma in a patient with history of mandibular ameloblastoma: A case report. Cancer Genet 2019;231–232:41–5.

27. Hammas N, Senhaji N, Alaoui Lamrani MY, et al. Astroblastoma - a rare and challenging tumor: a case report and review of the literature. J Med Case Rep 2018;12:102.

28. Agawa Y, Wataya T. The use of 5-aminolevulinic acid to assist gross total resection of pediatric astroblastoma. Childs Nerv Syst 2018;34:971–5.

29. Teleanu DM, Ilieşiu A, Bălaşa AF, et al. Astroblastoma - reviewing literature and one case report. Rom J Morphol Embryol 2018;59:1239–45.

30. Sadiq M, Ahmad I, Shuja J, et al. Astroblastoma in a young female patient: a case report and literature review of clinicopathological, radiological and prognostic characteristics and current treatment strategies. Brain Tumor Res Treat 2017;5:120–6.

31. Payne C, Batouli A, Stabingas K, et al. A pediatric tumor found frequently in the adult population: a case of anaplastic astroblastoma in an elderly patient and review of the literature. Case Rep Neurol Med 2017;2017:1607915.

32. Samples DC, Henry J, Yu FF, et al. A case of astroblastoma: Radiological and histopathological characteristics and a review of current treatment options. Surg Neurol Int 2016;7:S1008–12.

33. Narayan S, Kapoor A, Singhal MK, et al. Astroblastoma of cerebrum: a rare case report and review of literature. J Cancer Res Ther 2015;11:667.

34. de Castro FD, Reis F, Guerra JGG. Intraventricular mass lesions at magnetic resonance imaging: iconographic essay - part 2. Radiol Bras 2014;47:245–50.

35. Mellai M, Piazzi A, Casalone C, et al. Astroblastoma: beside being a tumor entity, an occasional phenotype of astrocytic gliomas? Onco Targets Ther 2015;8:451–60.

36. de la Garma VHE, Arcipreste AA, Vázquez FP, et al. High-grade astroblastoma in a child: report of one case and review of literature. Surg Neurol Int 2014;5:111.

37. Singh DK, Singh N, Singh R, et al. Cerebral astroblastoma: A radiopathological diagnosis. J Pediatr Neurosci 2014;9:45–7.

38. Barakat MI, Ammar MG, Salama HM, et al. Astroblastoma: case report and review of literature. Turk Neurosurg 2016;26:790–4.

39. Khosla D, Yadav BS, Kumar R, et al. Pediatric astroblastoma: a rare case with a review of the literature. Pediatr Neurosurg 2012;48:122–5.

40. Fu Y-J, Taniguchi Y, Takeuchi S, et al. Cerebral astroblastoma in an adult: an immunohistochemical, ultrastructural and genetic study. Neuropathology 2013;33:312–9.

41. Agarwal V, Mally R, Palande DA, et al. Cerebral astroblastoma: A case report and review of literature. Asian J Neurosurg 2012;7:98–100.

42. Bergkåsa M, Sundstrøm S, Gulati S, et al. Astroblastoma - a case report of a rare neuroepithelial tumor with complete remission after chemotherapy. Clin Neuropathol 2011;30:301–6.

43. Johnson KA, Bonnin JM, Boaz JC, et al. Anaplastic astroblastoma presenting as massive, sudden-onset, intraparenchymal hemorrhage. Pediatr Neurosurg 2010;46:457–61.

44. Turkmen E, Raisanen J, Dogan M, et al. A newborn with massive congenital astroblastoma. Fetal Pediatr Pathol 2011;30:325–8.

45. Binesh F, Akhavan A, Navabii H, Mehrabaniyan M. Anaplastic astroblastoma: a rare glial tumour. BMJ Case Rep 2011;2011:bcr0620114323.

46. Kemerdere R, Dashti R, Ulu MO, et al. Supratentorial high grade astroblastoma: report of two cases and review of the literature. Turk Neurosurg 2009;19:149–52.

47. Kantar M, Ertan Y, Turhan T, et al. Anaplastic astroblastoma of childhood: aggressive behavior. Childs Nerv Syst 2009;25:1125–9.

48. Eom K-S, Kim J-M, Kim T-Y. A cerebral astroblastoma mimicking an extra-axial neoplasm. J Korean Neurosurg Soc 2008;43:205–8.

49. Ganapathy S, Kleiner LI, Mirkin DL, et al. Unusual manifestations of astroblastoma: a radiologic-pathologic analysis. Pediatr Radiol 2009;39:168–71.

50. Fathi A-R, Novoa E, El-Koussy M, et al. Astroblastoma with rhabdoid features and favorable long-term outcome: report of a case with a 12-year follow-up. Pathol Res Pract 2008;204:345–51.

51. Unal E, Koksal Y, Vajtai I, et al. Astroblastoma in a child. Childs Nerv Syst 2008;24:165–8.

52. Bannykh SI, Fan X, Black KL. Malignant astroblastoma with rhabdoid morphology. J Neurooncol 2007;83:277–8.

53. Tumialán LM, Brat DJ, Fountain AJ, et al. An astroblastoma mimicking a cavernous malformation: case report. Neurosurgery 2007;60:E569–70.

54. Alaraj A, Chan M, Oh S, et al. Astroblastoma presenting with intracerebral hemorrhage misdiagnosed as dural arteriovenous fistula: review of a rare entity. Surg Neurol 2007;67:308–13.

55. Kaji M, Takeshima H, Nakazato Y, et al. Low-grade astroblastoma recurring with extensive invasion. Neurol Med Chir 2006;46:450–4.

56. Hata N, Shono T, Yoshimoto K, et al. An astroblastoma case associated with loss of heterozygosity on chromosome 9p. J Neurooncol 2006;80:69–73.

57. Kubota T, Sato K, Arishima H, et al. Astroblastoma: immunohistochemical and ultrastructural study of distinctive epithelial and probable tanycytic differentiation. Neuropathology 2006;26:72–81.

58. Lau PPL, Thomas TMM, Lui PCW, et al. "Low-grade" astroblastoma with rapid recurrence: a case report. Pathology 2006;38:78–80.

59. Kim DS, Park SY, Lee SP. Astroblastoma: a case report. J Korean Med Sci 2004;19:772–6.

60. Caroli E, Salvati M, Esposito V, et al. Cerebral astroblastoma. Acta Neurochir 2004;146:629–33.

61. Sener RN. Astroblastoma: diffusion MRI, and proton MR spectroscopy. Comput Med Imaging Graph 2002;26:187–91.

62. Port JD, Brat DJ, Burger PC, et al. Astroblastoma: radiologic-pathologic correlation and distinction from ependymoma. AJNR Am J Neuroradiol 2002;23:243–7.

63. Singla N, Dhandapani SS, Kapoor A, et al. Hemorrhage in astroblastoma: An unusual manifestation of an extremely rare entity. J Clin Neurosci 2016;25:147–50.

64. Yuzawa S, Nishihara H, Tanino M, et al. A case of cerebral astroblastoma with rhabdoid features: a cytological, histological, and immunohistochemical study. Brain Tumor Pathol 2016;33:63–70.

65. Sabharwal P, Sadashiva N, Unchagi A, et al. Intraventricular Astroblastoma in an Infant: A Case Report and Review of the Literature. Pediatr Neurosurg 2015;50:325–9.

66. Nasit JG, Trivedi P. Recurrent low-grade astroblastoma with signet ring-like cells and high proliferative index. Fetal Pediatr Pathol 2013;32:284–92.

67. Miranda P, Lobato RD, Cabello A, Gómez PA, Martínez de Aragón A.Complete surgical resection of high-grade astroblastoma with long time survival: case report and review of the literature. Neurocirugia 2006;17:60–3.

68. Huhn SL, Yung Y, Cheshier S, et al. Identification of phenotypic neural stem cells in a pediatric astroblastoma. J Neurosurg 2005;103:446–50.

69. Kim B-S, Kothbauer K, Jallo G. Brainstem astroblastoma. Pediatr Neurosurg 2004;40:145–6.

70. Palled SR, Thimmaya N, Jagadheesan S, et al. Astroblastoma: a rare case report. J Radiother Pract 2016;15:107–10.

71. El Hag MIA, Hdeib A, Ciarlini PDSC, Cohen ML. Astroblastoma and other predominantly pediatric supratentorial papillary/epithelioid gliomas. AJSP Rev Rep 2013;18:244–52.

72. Kurwale NS, Agrawal D, Sharma BS. Astroblastoma: A radio-histological diagnosis. J Pediatr Neurosci 2008;3:160–2.

73. Louis DN, Perry A, Reifenberger G, et al. The 2016 World Health Organization classification of tumors of the central nervous system: a summary. Acta Neuropathol 2016;131:803–20.

74. Louis DN, Perry A, Wesseling P, et al. The 2021 WHO classification of tumors of the central nervous system: a summary. Neuro Oncol 2021;23:1231–51.

Figure legends

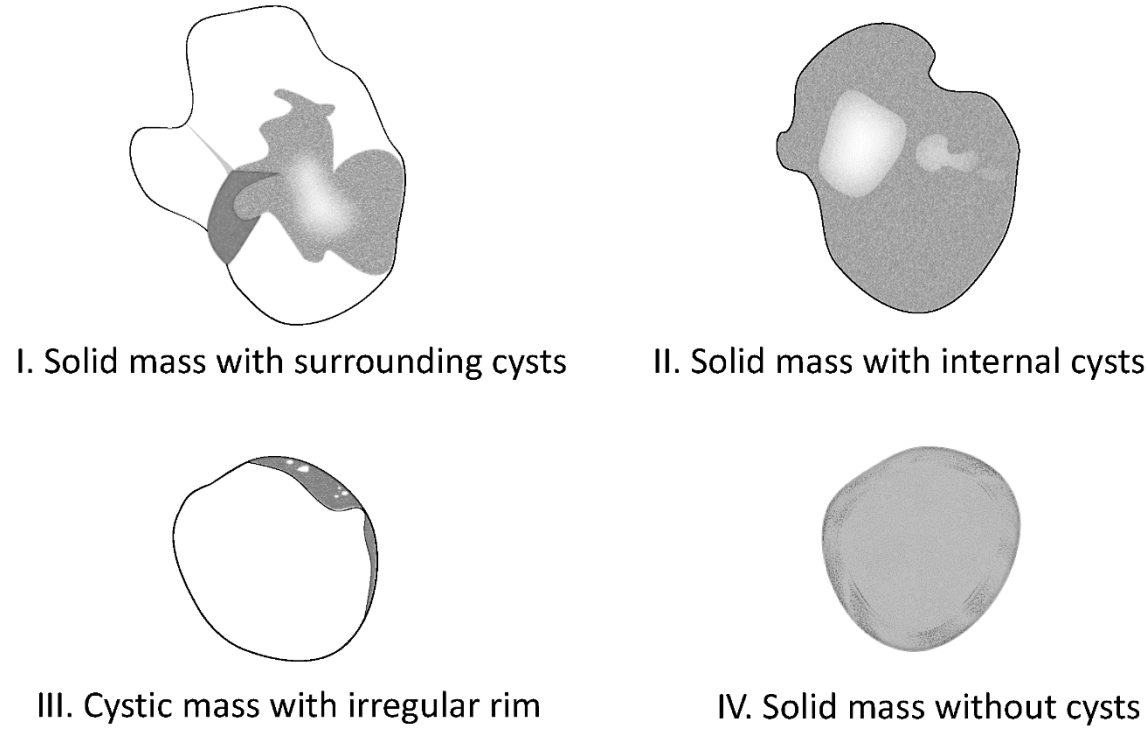

Figure 1. The four morphologies of astroblastoma.

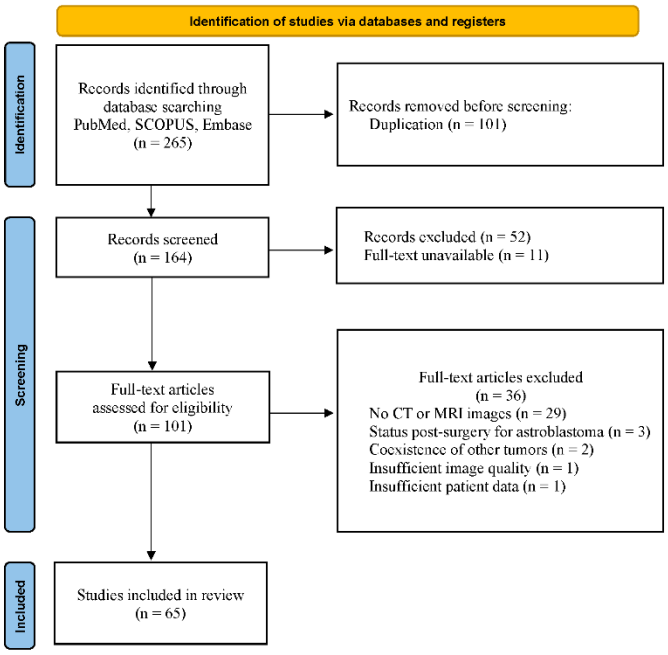

Figure 2. Flow diagram of study identification. n = number.

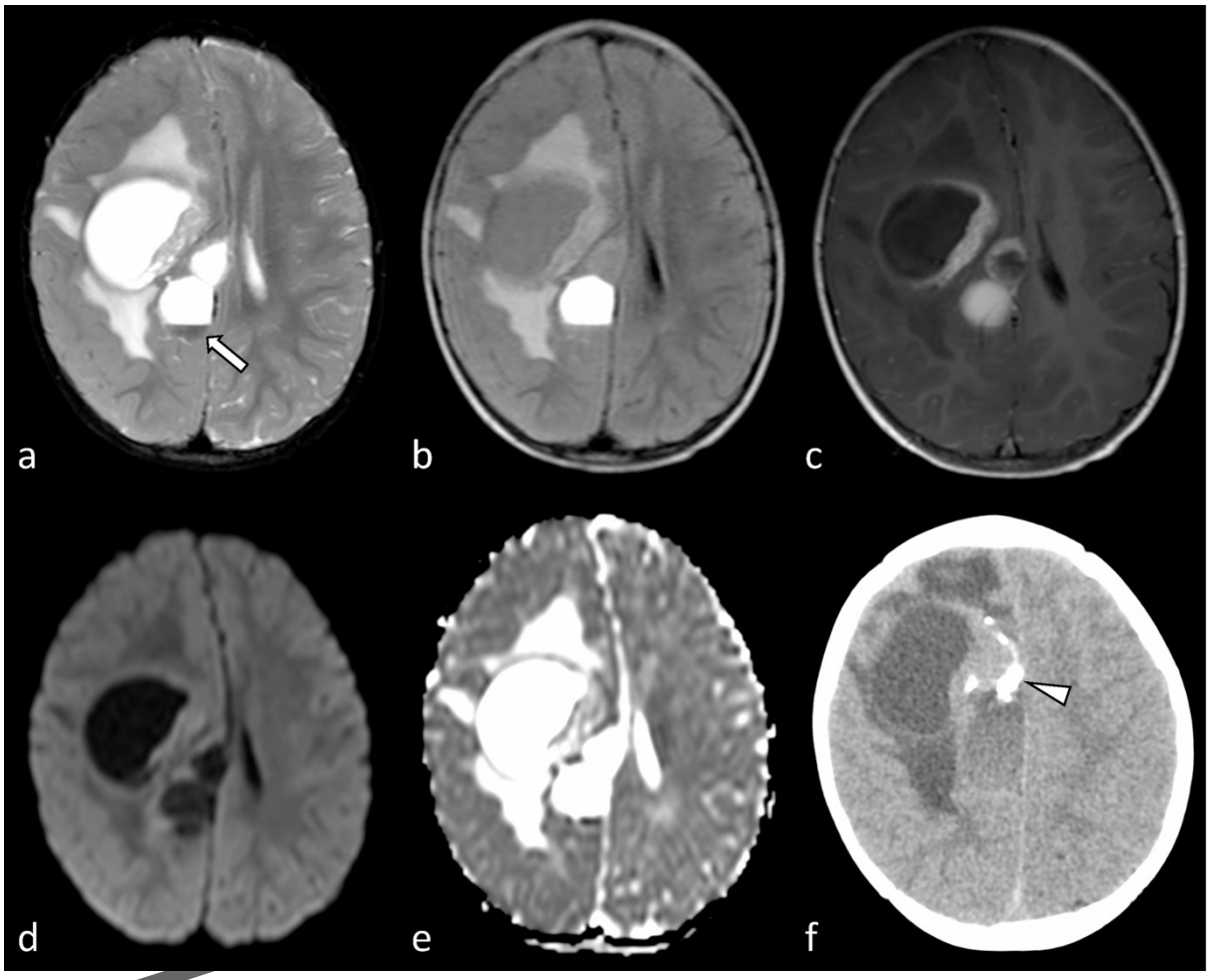

Figure 3. Supratentorial high-grade astroblastoma in a 1-year-old child presenting with weakness of the left upper and lower extremities (patient 1). The solid components of the tumor show high intensity on fat-suppressed T2-weighted image (a) and fluid-attenuated inversion recovery images (b) and low intensity on T1-weighted image (not shown) with heterogeneous enhancement (c). Diffusion restriction is observed with the mean apparent diffusion coefficient value of 0.81×10^{-3} mm^2/s (d, e). The cystic components show various signal intensities on

each sequence with a fluid-fluid level indicating intratumoral hemorrhage (a: arrows). Unenhanced CT shows an intratumoral calcification (f: arrowhead). The tumor appears as a solid mass with surrounding cysts (morphology I).

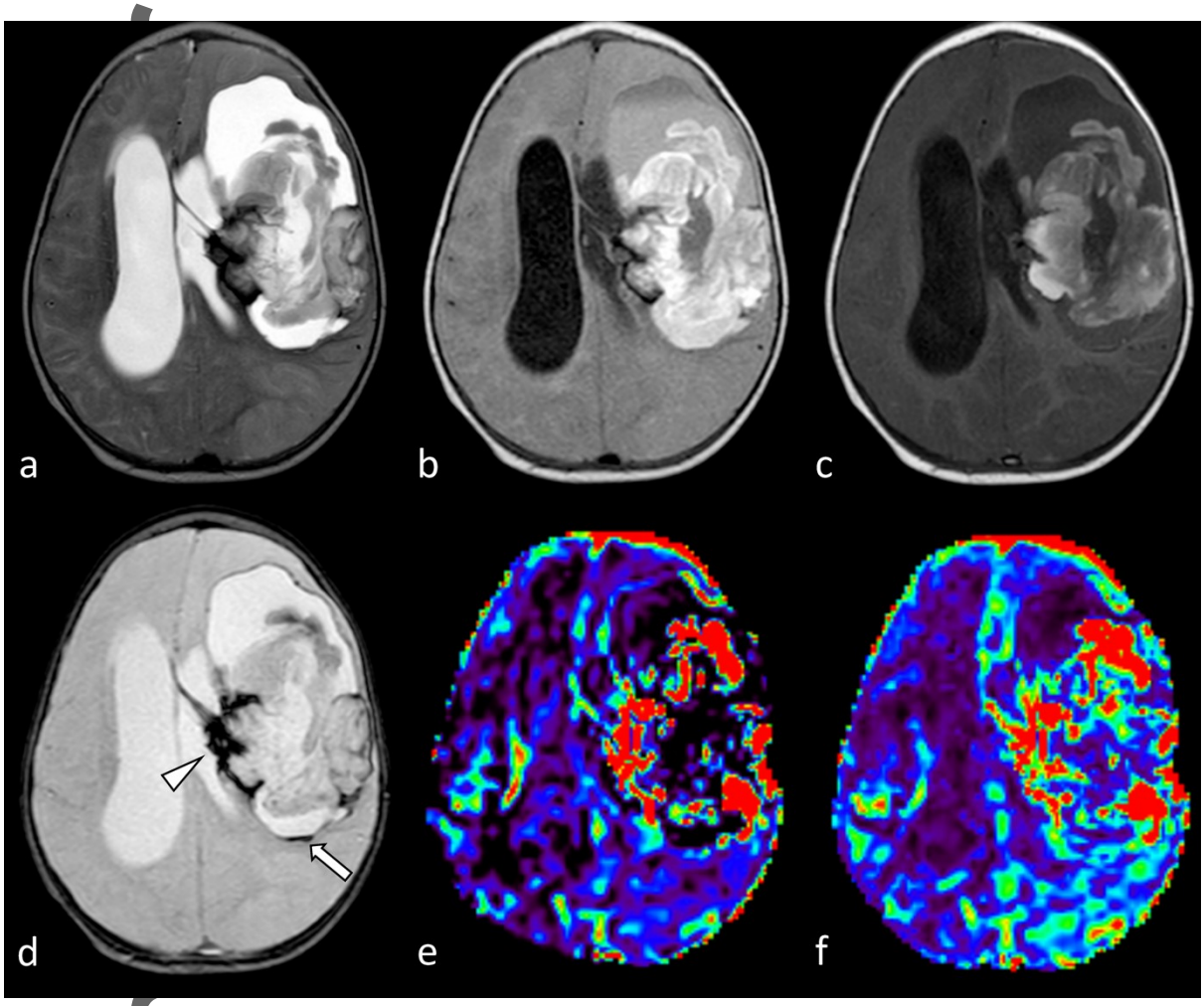

Figure 4. Supratentorial high-grade astroblastoma in a 7-month-old child presenting with eye rotation, fever, and vomiting (patient 8). The solid components of the tumor show mainly high intensity on T2-weighted image (a) and fluid-attenuated inversion recovery (FLAIR) images

(b), and high and iso-intensity on T1-weighted image (c). The cystic components show high intensity on T2-weighted image (a) and FLAIR images (b) and low intensity on T1-weighted image (c). A T2*-weighted image shows very low intensity, suggestive of intratumoral calcification (d: arrowhead) and a fluid-fluid level, indicating hemorrhage (d: arrow). The tumor presents as a solid mass with surrounding cysts (morphology I). Dynamic susceptibility contrast perfusion MRI shows elevated relative cerebral blood volume (e) and blood flow (f) in the solid components of the tumor.

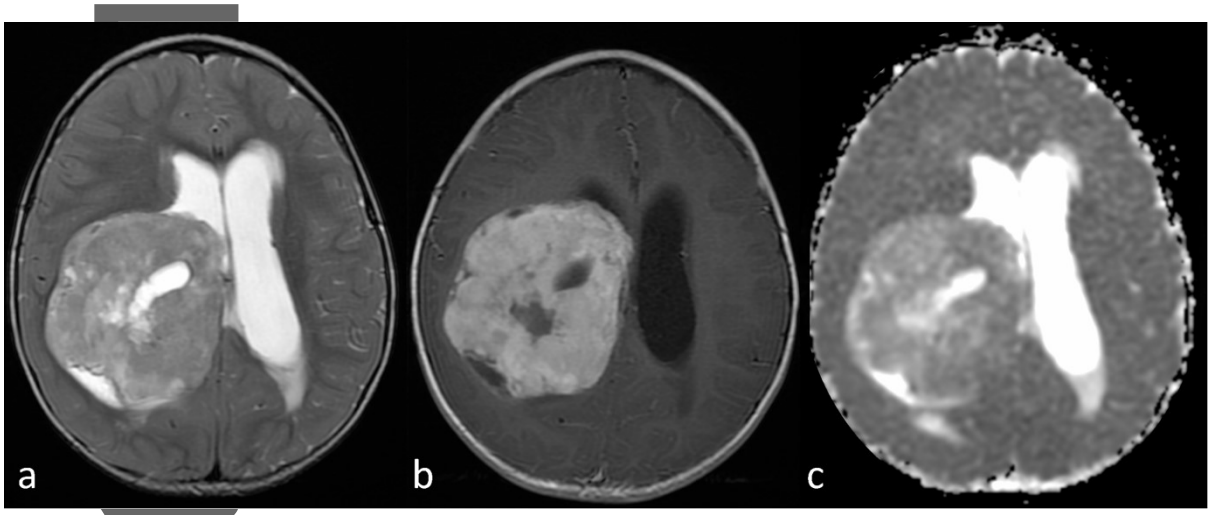

Figure 5. Supratentorial high-grade astroblastoma in a 1-year-old boy presenting with weakness of the left lower extremity (patient 7). The solid components of the tumor show high

intensity on T2-weighted image (a) and low intensity on T1-weighted image (not shown) with heterogeneous enhancement (b). The mean apparent diffusion coefficient value is 1.02 × $10^{-3}mm^2/s$ (c). The tumor shows a solid mass with internal cysts (morphology II).

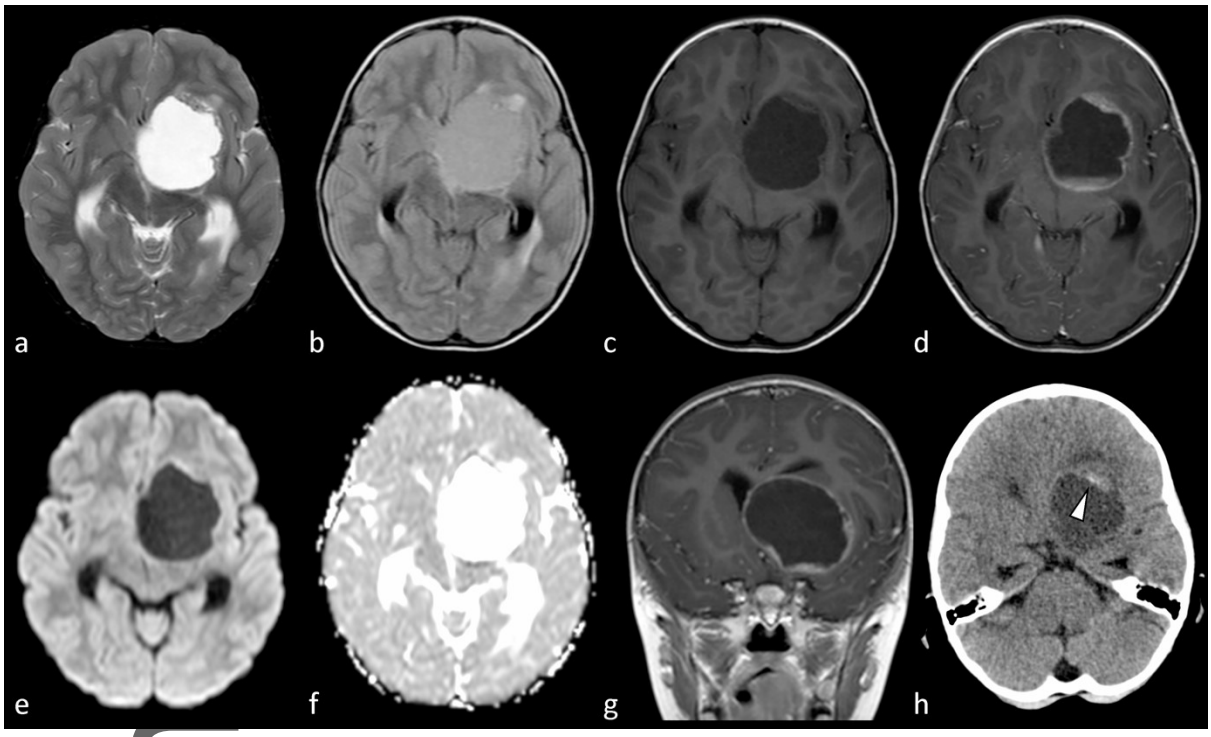

Figure 6. Supratentorial low-grade astroblastoma in a 3-year-old girl presenting with headache (patient 2). The solid components of the tumor show iso and low intensity on T2-weighted image (a), high intensity on fluid-attenuated inversion recovery image (b), and low intensity on

T1-weighted image (c) with heterogeneous enhancement (d). Diffusion restriction is observed with the mean apparent diffusion coefficient value of $0.65 \times 10^{-3}mm^2/s$ (e, f). The tumor shows a cystic mass with irregular rim (morphology III) and ependymal contact on post-contrast coronal T1-weighted image (g). Unenhanced CT shows partial calcification (h, arrowhead).

Tables

Table 1. Demographic, clinical, and radiological data of the eight patients with astroblastomas in our hospital

	Patients	1	2	3	4	5	6	7	8
Demographic & Clinical	Age at diagnosis (years)	1/Female	3/Female	30/Female	3/Female	12/Female	13/Female	1/Male	7 months/Female
	Presenting	LUE	Headache	Headache		Headache	Dizzin	LLE	Eye

data	complaint	and LLE weakness	che	che, Nausea/Vomiting		che, Nausea/Vomiting	ess, Loss of Vision	weakness	rotation, Fever up, Vomiting
	Tumor grade	High	High	Low		High	High	High	High
	Surgery	Yes	Yes	Yes	Yes	Yes	Yes	Yes	
	Chemotherapy	Yes	No	No	Yes	Yes	No	Yes	
	Radiation	No	Yes	No	Yes	Yes	No	No	Autopsy
	Recurrence, period (from surgery)	No	No	No	N/A	45 months	35 months	8 months	
	Patient status	Survive	Survive	Survive	Deceased	Survive	Survive	Survive	Deceased

	Follow up duration (from surgery)	100 months	103 months	135 months	1 month	71 months	109 months	9 months	N/A
	Size (mm)	60 × 49 × 45	49 × 46 × 42	33 × 35 × 30	72 × 62 × 57	51 × 42 × 49	62 × 45 × 53	59 × 64 × 72	90 × 64 × 67
	Laterality	Right	Left	Right	Left	Right	Right	Right	Left
Radiological data	Tumor extension	Frontoparietal	Frontal, Basal ganglia	Temporal	Frontoparietal, Basal ganglia	Frontal	Parietotoccipital	Lateral ventricle	Frontoparietal
	Tumor margin	Well	Well	Well	Well	Well	Well	Well	Well
	Morphology	I	III	I	II	II	I	II	I

MRI signal intensity (solid)	T2WI	High	Iso & Low	High & Iso		High	High & Low	High	High
	FLAIR	High	High	High & Iso	High	High & Iso	High & Low	Iso	High
	T1WI	Iso	Low	Low	Low	Iso & Low	Low	Low	HIgh
MRI signal intensity (cystic)	T2WI	High & Low	High	High & Iso		High	High & Low	High	HIgh
	FLAIR	High & Low	Low	High & Iso	High	High	High & Low	High	High
	T1WI	High	Low	Low	High	Low	Iso &	High	Low

I & Low				low			
Diffusion restriction	Yes	Yes	No	Yes		No	Yes
ADC value (10^{-3} mm^2/s)	0.81	0.65	1.27	0.69		1.02	0.64
Contrast enhancement	Hetero geneous	Hetero geneous	Hetero geneous	Scarce	Hetero geneous	Hetero geneous	Hetero geneous	Hetero geneous
Peritumoral edema	Yes	Yes	Yes	No	Yes	No	No	No
CT (solid/cystic)	High / Low	Iso / Low			High / Low			High / Low
Calcification	Yes	Yes	Yes	Yes	Yes		Yes	Yes
Hemorrhage	Yes	No		Yes	No			Yes

Leptomeninge al contact	Yes	No	Yes	Yes	Yes	Yes	No	Yes
Ependymal contact	No	Yes	No	Yes	Yes	Yes	Yes	Yes

LUE = left upper extremity, LLE = left lower extremity, T1/T2WI: T1/T2-weighted images. FLAIR: fluid-attenuated inversion recovery, Iso = iso intensity/ iso attenuation, ADC = apparent diffusion coefficient, N/A = Not applicable

Table 2. Demographic and clinical information of the 79 patients with astroblastomas

Demographic	
Median age at diagnosis (years [range])	13 [0–77]
Sex	Male = 17, Female = 62

Clinical	
Headache	Headache: 51/75 (68.0%); Nausea/Vomiting: 22/75 (29.3%); Seizure/epilepsy: 20/75 (26.7%)
Tumor grade	Low = 36/71 (50.7%), High = 35/71 (49.3%)
Treatment strategy	
Surgery alone	44/76 (57.9%)
Surgery and radiation	14/76 (18.4%)
Surgery and chemotherapy	2/76 (2.6%)
Surgery and chemoradiation	13/76 (17.1%)
Chemotherapy alone	1/76 (1.3%)
Chemotherapy and radiation	1/76 (1.3%)
Autopsy	1/76 (1.3%)
Recurrence after gross total resection	16/56 (28.6%)

Patient status	Survive = 58/68 (85.3%), Deceased = 10/68 (14.7%)
Follow up duration (median [range]) (n = 61)	18 months [<1–135]

n = number

Table 3. Neuroimaging characteristics of the 79 patients with astroblastomas

Parameters	
Size (median [range]) (n = 38)*	57.5 mm [25–110]
Laterality	Right, 38/79 (48.1%); Left, 33/79 (41.8%); Middle, 7/79 (8.9%); Bilateral, 1/79 (1.3%)
Tumor extension	
Supratentorial	74/79 (93.7%)
Frontal lobe	44/79 (55.7%)

Parietal lobe	33/79 (41.8%)	
Temporal lobe	11/79 (13.9%)	
Insula	3/79 (3.8%)	
Basal ganglia	4/79 (5.1%)	
Corpus callosum	2/79 (2.5%)	
Ventricle	4/79 (5.1%)	
Extra-axial (except for ventricles)	1/79 (1.3%)	
Brainstem	4/79 (5.1%)	
Cerebellum	1/79 (1.3%)	
Tumor margin	well-defined = 61/79 (77.2%), ill-defined = 18/79 (22.8%)	
Tumor morphology	I: 24/79 (30.4%); II: 40/79 (50.6%); III: 8/79 (10.1%); IV: 7/79 (8.9%)	
T2WI signal intensity	Solid component	Cystoid component

High intensity	34/53 (64.2%)	45/46 (97.8%)
Iso intensity	16/53 (30.2%)	0
Low intensity	20/53 (37.7%)	3/46 (6.5%)
FLAIR signal intensity	Solid component	Cystoid component
High intensity	18/28 (64.3%)	16/25 (64.0%)
Iso intensity	10/28 (35.7%)	1/25 (4.0%)
Low intensity	7/28 (25.0%)	10/25 (40.0%)
T1WI signal intensity	Solid component	Cystoid component
High intensity	10/30 (33.3%)	6/28 (21.4%)
Iso intensity	7/30 (23.3%)	1/28 (3.6%)
Low intensity	17/30 (56.7%)	23/28 (82.1%)
Contrast enhancement		
Any	63/64 (98.4%)	

Heterogeneous	44/64 (68.8%)	
Homogeneous	16/64 (25.0%)	
Ring	1/64 (1.6%)	
Scarce	2/64 (3.1%)	
Diffusion restriction	9/14 (64.3%)	
Median ADC value ($10^{-3}mm^2/s$) [range] (n = 8)	0.69 [0.47–1.3]	
Peritumoral edema	54/77 (70.1%)	
CT density	Solid component	Cystoid component
High attenuation	23/27 (85.2%)	0
Iso attenuation	2/27 (7.4%)	0
Low attenuation	3/27 (11.1%)	26/26 (100%)
Calcification; Hemorrhage	21/30 (70.0%); 12/23 (52.2%)	

Leptomeningeal contact;	61/76 (80.3%); 31/67 (46.3%)
Ependymal contact	

* In cases where measurements in multiple directions were performed, the maximum value was used for the calculation of the tumor diameter. n = number, T1/T2WI = T1/T2-weighted images, FLAIR = fluid-attenuated inversion recovery, ADC = apparent diffusion coefficient.

Table 4. Inter-reader reliability

	kappa	ICC
Maximum tumor size (mm)*		0.99
ADC value (10^{-3} mm^2/s)*		0.99
Laterality	1	
Tumor extension	1	
Tumor margin	0.9	

Morphology		0.94
MRI signal intensity (solid)	T2WI	0.90
	FLAIR	0.66
	T1WI	0.85
MRI signal intensity (cystic)	T2WI	0.79
	FLAIR	0.86
	T1WI	0.73
Diffusion restriction		1
Contrast enhancement		0.86
Peritumoral edema		0.94
CT solid		0.70
CT cystic		1
Calcification		0.96

Hemorrhage	0.94
Leptomeningeal contact	1
Ependymal contact	1

* ICC of tumor size and ADC value were calculated in the eight cases from our hospital.

ICC = intraclass correlation coefficient, T1/T2WI = T1/T2-weighted images, FLAIR = fluid-attenuated inversion recovery, ADC = apparent diffusion coefficient.

Table 5. Statistical analysis

	High-grade	Low-grade	P-values
Median age at diagnosis (years [range])	12 (0–77) (35 patients)	14 (0–54) (36 patients)	0.86

Recurrence after gross total resection	7/24 (29.2%)	8/29 (27.6%)	>0.99
Ill-defined margin	8/35 (22.9%)	7/36 (19.4%)	0.78
Typical morphology	33/58 (56.9%)	2/13 (15.4%)	0.012*

*Statistically significant